Low Interfacial Toughness Materials for Effective Large-Scale De-Icing

Kevin Golovin[1,2†], Abhishek Dhyani[2,3†], M. D. Thouless[1,4*], and Anish Tuteja[1,2,3,5*]

[1]Department of Materials Science and Engineering, [2]Biointerfaces Institute, [3]Macromolecular Science and Engineering, [4]Department of Mechanical Engineering, [5]Department of Chemical Engineering, University of Michigan – Ann Arbor. * indicates corresponding author. † these authors contributed equally to this work.

Abstract: Ice accretion has adverse effects on a range of commercial and residential activities. The force required to remove ice from a surface is typically considered to scale with the iced area. This imparts a scalability limit to the use of icephobic coatings for structures with large surface areas, such as power lines or ship hulls. We describe a class of materials that exhibit a low interfacial toughness with ice, resulting in systems for which the forces required to remove large areas of ice (few cm^2 or greater) are both low and independent of the iced area. We further demonstrate that coatings made of such materials allow ice to be shed readily from large areas (~$1m^2$) merely by self-weight.

One Sentence Summary: Reducing interfacial toughness allows for removal of ice over large areas using less force.

Main Text: The accretion of ice on surfaces can have a severe detrimental impact on a range of commercial and residential activities *(1)*. Consequently, there has been an effort to create coatings that protect against the build-up of ice. Typically, the efficacy of these coatings has been evaluated by measuring the force, F, to debond a specified area, A, of ice, and defining an ice-adhesion strength $\tau_{ice} = F/A$ as the characteristic property for the system (*2*). The term

icephobic is generally used to describe surfaces for which $\tau_{ice} < 100$ kPa *(3, 4)*, in comparison to structural materials such as aluminum and steel for which $\tau_{ice} > 1000$ kPa *(2, 5, 6)*.

Using τ_{ice} to characterize an interface inevitably requires that the force necessary to remove ice scales with the iced area. Many engineering structures susceptible to icing, such as airplane wings, wind-turbine blades *(7)*, and boat hulls *(8)* have surface areas that can approach thousands of square meters. Consequently, even with extremely icephobic coatings, structures with large surface areas would require prohibitively high forces to detach entire sheets of ice from the surface. In this work, we develop low-interfacial-toughness (LIT; interfacial toughness $\Gamma < 1$ J/m^2) materials for which the force required to remove adhered ice from large areas (few cm^2 or greater) is both low and independent of interfacial area.

An interfacial cohesive strength, as represented by the ice-adhesion strength, is one way to describe the bonding across an interface *(9)*. A countervailing perspective on fracture *(10, 11)* is that an interface should be described in terms of its bonding energy (or, more correctly, its toughness). Further, while the work of adhesion is often discussed in connection to ice adhesion, it is the strength that is generally used to describe failure *(1, 2, 4)*. This is true whether the adhesion is viewed in terms of surface energy *(3, 12, 13)*, interfacial cavitation *(14)*, or lubrication *(15-17)*.

The two competing perspectives for delamination, strength and toughness, can be rationalized by means of cohesive-zone models of fracture *(18-22)*. Simple analytical models (see Section 2A, 2B in *(23)*) can be used to demonstrate that the shear strength of the interface, $\hat{\tau}$, controls delamination when the length of the interface is relatively small, so that $\tau_{ice} = \hat{\tau}$. This is manifested by a spontaneous rupture along the entire interface (Movie S1). Conversely, Γ

controls delamination when the length of the interface is relatively large. This is manifested by the propagation of an interfacial crack (Movie S1). The analysis shows that there is a critical bonded length at which a transition between the two modes of failure occurs, given by $L_c = \sqrt{2E_{ice}\Gamma h / \hat{\tau}^2}$, where E_{ice} is the modulus of ice (≈ 8.5 GPa) of thickness *h*. In this context, ice is not a ductile material even close to its melting temperature, and treating it as an elastic solid, at the engineering strain rates and time scales relevant here, is a reasonable approach *(11),* provided $\frac{2E_{ice}\Gamma}{\sigma_Y^2} < h < L$, where σ_Y is the yield strength of ice. Importantly, when $L > L_c$, the force required to delaminate the ice is constant, no matter how large the interface may be.

We first verified the concept that the force required to remove an ice layer reaches an asymptotic value if the interface is long enough. This was done using substrates made from common plastics such as polyethylene, polypropylene, and polystyrene (substrate thickness t = 1.6 mm; see Table 1) without any additional modification. We used a setup similar to those reported previously (*2, 14, 24*), but instead of using relatively short lengths, corresponding to a few millimeters of bonded ice (*2, 14, 24-26*), we designed our apparatus so that much longer interfaces could be evaluated (insets Fig. 1C, 1D, see section 1B in *(23)*). Plots showing the force (per unit width) necessary to detach the ice, $\tilde{F}_{ice}$ as a function of the bonded length, *L*, are shown in Figures S7-S12. For the most part, we observed that $\tilde{F}_{ice}$ increased proportionally to *L*, only when *L* was small. Beyond the transition length, L_c, no additional force was necessary to dislodge the ice. The corresponding asymptotic force, $\tilde{F}_{ice}^{cr}$, can be used to determine the interfacial toughness, Γ, from $\Gamma = (\tilde{F}_{ice}^{cr})^2 / 2E_{ice}h$ (*27-29*). Specific examples of this behavior are

shown in Fig. 1A for ice bonded to four different plastic substrates, each of which has a transition length less than 10 cm.

We repeated this experiment for aluminum substrates coated with different icephobic coatings ($t \approx 1$ mm; see Fig. 1B). These coatings were all based on polydimethylsiloxane (PDMS) rubber, which has been studied for its low ice-adhesion properties enabled via lubrication (*25*), interfacial cavitation (*14, 24*), low surface energy (*30, 31*), and interfacial slippage (*32, 33*). In contrast to the plastic substrates, these materials did not exhibit a toughness-controlled regime of delamination within the range of bonded lengths studied.

A low interfacial-shear-strength does not necessarily imply a low toughness. Thus, a material that debonds from ice more readily than another if the interface is short, does not necessarily debond more readily if the interface is long. This can be seen by comparing the results for polyvinylchloride and polyamide in Fig. 1A or the results for polypropylene (Fig. 1A) with Silicone B (Fig. 1B). The shear strength of the interface between ice and polypropylene substrate can be calculated from the initial slope of the line in Fig. 1A as $\hat{\tau} = 320 \pm 40$ kPa. The shear strength of the interface between ice and Silicone B coating is an order of magnitude lower, being equal to $\hat{\tau} = 29 \pm 2$ kPa. However, as can be seen in Fig. 1C, the force for detachment continually increases for Silicone B, even out to 100 cm. For interfaces longer than 50 cm, the ice is removed more easily from polypropylene ($\Gamma = 1.9$ J/m^2) than it is from the Silicone B ($\Gamma > 9$ J/m^2) coating.

These data can be re-expressed in terms of the apparent ice-adhesion strengths for the two interfaces, by dividing the force by the initial bonded area (Fig. 1D). As such, the apparent ice-adhesion strength, for a length of 100 cm for polypropylene ($\tau_{ice} \approx 12$ kPa), was less than half

that of the icephobic PDMS ($\tau_{ice} \approx 29$ kPa), although the true ice adhesion strength $\hat{\tau}$ was an order of magnitude greater (Fig. 1D). Over the last decade, achieving $\tau_{ice} < 15$ kPa has necessitated the use of either soft rubbers (*14, 24*) or highly lubricated systems (*25, 26, 32*), which can suffer from poor durability (*14*). However, here we show that one can obtain much lower values of apparent ice adhesion strength for large structures by selecting a material with a low toughness.

There are several contributions to interfacial toughness. One is associated with the bonding energy between the ice and the coating. A lower bound on this energy would be about 0.1 J/m^2, corresponding to van-der-Waals interactions (*5, 34*). An additional contribution could come from localized losses within the coating, associated with the high-stress region at the crack tip. These two effects would be classically considered to be contributing to interfacial toughness. However, if the process of delamination causes deformation of the coating, then the strain energy associated with this deformation must also be considered as a contribution to the effective toughness, Γ, between the ice and substrate. From a cohesive-zone perspective, one can consider the toughness of an interface to be given by the area under the force-displacement curve of the entire interface, including the coating (*18, 19*). Therefore, assuming linear elasticity, this contribution to the toughness can be estimated as $\Gamma \approx \hat{\tau}^2 t / 2G$, where G is the shear modulus and t is the thickness of the coating (see section 2C in *(23)*, Fig. S6). Consequently, it should be possible to minimize the effective toughness by minimizing the thickness of a polymeric coating.

To investigate this concept, we varied the thickness of PVC films and confirmed that Γ scaled with the coating thickness, t (Fig. 2A). Lowering t from 150 μm to 2 μm (see section 1A in *(23)*), reduced the Γ from ~ 3 J/m^2 to 2 J/m^2. Previous work (*14, 35*) has shown that for

icephobic elastomers $\hat{\tau} \propto t^{1/2}$. Therefore, the design of LIT ($\Gamma < 1$ J/m^2) materials can be significantly different than the design of icephobic materials. Icephobic surfaces can be made more effective as t increases, while LIT surfaces become more effective as t decreases.

To further reduce Γ, we explored the effects of plasticizing the PVC with medium-chain triglyceride oil (MCT; see section 1A in *(23)*). Figure 2A shows the general drop in toughness observed with increased plasticization. As shown in Fig. 2B, the additional drop in shear strength associated with the addition of 50% MCT was large enough for the transition length to become too long for the toughness to be measured for the thicker coatings. The general trends between strength, toughness, coating thickness, and level of plasticization can be seen in Figs. 2C, 2D.

By optimizing the thickness and plasticizer content within the PVC, we were able to fabricate LIT materials exhibiting Γ as low as 0.27 J/m^2 ($\tilde{F}_{ice}^{cr} = 52 \pm 7$ N/cm). Similarly, by optimizing the thickness and plasticizer content, we fabricated LIT polystyrene (20 wt% diisodecyl adipate, Table 1, section 1A in *(23)*, Fig. S18) with $\Gamma \approx 0.43$ J/m^2 ($\tilde{F}_{ice}^{cr} = 66 \pm 6$ N/cm), and LIT PDMS (40 wt% silicone oil, Table 1) that displayed an even lower $\Gamma \approx 0.12$ J/m^2 ($\tilde{F}_{ice}^{cr} = 35 \pm 4$ N/cm).

We coated 1.2-meter-long aluminum beams with these LIT PVC and LIT PDMS coatings (with a nominal thickness of $t \approx 1$ - 2 μm, see section 1B in *(23)*), and conducted large-scale testing inside a walk-in freezer at -10 °C. Fig. 2E shows that the force of detachment did not increase for $L > L_c$, even over one meter of interfacial length ($\tilde{F}_{ice}^{cr} = 52 \pm 7$ N/cm for LIT PVC and $\tilde{F}_{ice}^{cr} = 35 \pm 4$ N/cm for LIT PDMS). These correspond to values of $\tau_{ice} < 6$ kPa and < 4 kPa,

for the LIT PVC and LIT PDMS surfaces, respectively. In contrast, for aluminum coated with an extremely soft, icephobic PDMS rubber (plasticized Silicone B, $\hat{\tau} = 12$ kPa), we measured $\tilde{F}_{ice} = 126$ N/cm at $L = 100$ cm. Additional experiments confirmed that we were not observing delamination (Fig. S3) or cohesive failure (Fig. S5) of the LIT coatings during ice removal.

For a given ice thickness, there will always be an interfacial length beyond which LIT materials require less force than icephobic materials to remove the adhered ice (Fig. S19). As an example, to mimic the deicing of power line cables, we conducted off-center loaded beam tests by flexing 1.2 meter-long uncoated, and coated (with both icephobic and LIT coatings) aluminum beams, with ice adhered on one side (see section 1B in *(23)*). The icephobic (Silicone B; $t \approx 1$ mm) and LIT (Silicone B + 40 wt% silicone oil; $t \approx$ 1-2 μm) coatings were fabricated using the same polymer, PDMS, but the icephobic PDMS system exhibited low interfacial strength ($\Gamma >$ 8.82 J/m^2 and $\hat{\tau} = 30$ kPa), whereas the LIT PDMS exhibited low interfacial toughness ($\Gamma = 0.12$ J/m^2 and $\hat{\tau} = 115$ kPa). Upon flexing, ice fractured cleanly from the LIT PDMS at a low deflection of 2.4 cm from the center of the beam (Fig. 3A). Both the uncoated and icephobic-coated beams displayed no significant signs of ice detachment even at an extreme deflection of ~ 35 cm (Movie S2). To mimic the deicing of an airplane via wing tip deflection, end-loaded cantilever beam tests were conducted (Fig. S20, Movie S3). The deflection necessary to remove the ice adhered to the LIT coating was an order of magnitude less than that of the icephobic or uncoated surfaces. The LIT coating also enables the removal of ice from complex geometries, such as an ice-cube tray (Fig. S17 and Movie S4), with little to no force.

The isothermal freezing conditions within a freezer (data shown in Fig. 1C, 1D, 2E, 3A) differ from those experienced in Peltier-plate based systems (data shown in Fig. 1, 2, 2E), in

which ice is formed via unidirectional cooling from the surface. Ice formation conditions, particularly ambient temperature, can significantly affect the structure / interfacial properties for ice (*1, 36-38*). The similitude of our data for $L \leq 20$ cm (Peltier) and $L > 20$ cm (freezer; see Figs. 1C, 1D, 2E, 3A) lengths of ice indicated that LIT materials can be effective in shedding ice in different ice formation conditions. Additionally, we measured $\hat{\tau}$, $\tilde{F}_{ice}^{cr}$, and Γ values for polypropylene and low interfacial toughness PDMS at -20 ºC, -10 ºC and -5 ºC. The values of these interfacial properties (Fig. S4), for both the LIT-PDMS and polypropylene, appear to be invariant with temperature and the different ice-formation conditions, within the ranges studied.

To evaluate a third ice formation condition, we coated a 1 m x 1 m Al panel with our LIT PDMS and allowed ice to form outside at -7 °C overnight (see section 1E in *(23)*, Fig. 3B). Once fully frozen, we observed that the weight of the ice at a thickness of 1 cm was enough to completely and cleanly remove the attached ice (Movie S5). This yielded $\tau_{ice} = 0.09$ kPa. Whereas varying icing conditions can lead to tensile cracking and subsequent fragmentation of the ice, as long as the fragmented length remains greater than L_c, LIT materials will remain an effective means of ice removal.

References and Notes:

1. L. Makkonen, Ice adhesion—theory, measurements and countermeasures. *Journal of Adhesion Science and Technology* **26**, 413-445 (2012).
2. A. J. Meuler *et al.*, Relationships between water wettability and ice adhesion. *ACS applied materials & interfaces* **2**, 3100-3110 (2010).
3. V. Hejazi, K. Sobolev, M. Nosonovsky, From superhydrophobicity to icephobicity: forces and interaction analysis. *Scientific reports* **3**, 2194 (2013).
4. H. Sojoudi, M. Wang, N. D. Boscher, G. H. McKinley, K. K. Gleason, Durable and scalable icephobic surfaces: similarities and distinctions from superhydrophobic surfaces. *Soft Matter* **12**, 1938-1963 (2016).
5. R. Menini, M. Farzaneh, Advanced Icephobic Coatings. *Journal of Adhesion Science and Technology* **25**, 971-992 (2011).
6. N. D. Mulherin, R. B. Haehnel, "Ice Engineering: Progress in Evaluating Surface Coatings for Icing Control at Corps Hydraulic Structures," (Engineer research and development center, Hanover, NH, Cold Regions Research and Engineering Lab, 2003).
7. T. Burton, I. Books24x, *Wind energy handbook, second edition*. (John Wiley & Sons Ltd, Chichester, West Sussex, U.K., 2011).
8. F. M. White, *Viscous fluid flow*. (McGraw-Hill, New York, 1991).
9. C. E. Inglis, Stresses in a plate due to the presence of cracks and sharp corners. *Proceedings of the Institute of Naval Architects* **55**, 219-230 (1913).
10. A. A. Griffith, The phenomena of rupture and flow in solids. (1921).
11. H. J. Frost, M. F. Ashby, *Deformation mechanism maps: the plasticity and creep of metals and ceramics*. (Pergamon press, 1982).
12. S. A. Kulinich, M. Farzaneh, Ice adhesion on super-hydrophobic surfaces. *Applied Surface Science* **255**, 8153-8157 (2009).
13. K. K. Varanasi, T. Deng, J. D. Smith, M. Hsu, N. Bhate, Frost formation and ice adhesion on superhydrophobic surfaces. *Applied Physics Letters* **97**, 234102 (2010).
14. K. Golovin *et al.*, Designing durable icephobic surfaces. *Science Advances* **2**:e1501496 (2016).
15. P. Kim *et al.*, Liquid-infused nanostructured surfaces with extreme anti-ice and anti-frost performance. *ACS Nano* **6**, 6569-6577 (2012).
16. J. Chen *et al.*, Robust prototypical anti-icing coatings with a self-lubricating liquid water layer between ice and substrate. *ACS applied materials & interfaces* **5**, 4026-4030 (2013).
17. Y. H. Yeong, A. Milionis, E. Loth, J. Sokhey, Self-lubricating icephobic elastomer coating (SLIC) for ultralow ice adhesion with enhanced durability. *Cold Regions Science and Technology* **148**, 29-37 (2018).
18. R. B. Sills, M. D. Thouless, Cohesive-length scales for damage and toughening mechanisms. *International Journal of Solids and Structures* **55**, 32-43 (2015).
19. R. B. Sills, M. D. Thouless, The effect of cohesive-law parameters on mixed-mode fracture. *Engineering Fracture Mechanics* **109**, 353-368 (2013).
20. J. Parmigiani, M. Thouless, The effects of cohesive strength and toughness on mixed-mode delamination of beam-like geometries. *Engineering Fracture Mechanics* **74**, 2675-2699 (2007).
21. K. Kendall, Shrinkage and peel strength of adhesive joints. *Journal of Physics D: Applied Physics* **6**, 1782 (1973).

22. A. Hillerborg, M. Modéer, P.-E. Petersson, Analysis of crack formation and crack growth in concrete by means of fracture mechanics and finite elements. *Cement and concrete research* **6**, 773-781 (1976).
23. See supplementary materials.
24. D. L. Beemer, W. Wang, A. K. Kota, Durable gels with ultra-low adhesion to ice. *Journal of Materials Chemistry A* **4**, 18253-18258 (2016).
25. C. Urata, G. J. Dunderdale, M. W. England, A. Hozumi, Self-lubricating organogels (SLUGs) with exceptional syneresis-induced anti-sticking properties against viscous emulsions and ices. *J. Mater. Chem. A* **3**, 12626-12630 (2015).
26. P. Irajizad, M. Hasnain, N. Farokhnia, S. M. Sajadi, H. Ghasemi, Magnetic slippery extreme icephobic surfaces. *Nature Communications* **7**, 13395 (2016).
27. M. D. Thouless, Cracking and delamination of coatings. *Journal of Vacuum Science & Technology A: Vacuum, Surfaces, and Films* **9**, 2510-2515 (1991).
28. Z. Suo, J. W. Hutchinson, Interface crack between two elastic layers. *International Journal of Fracture* **43**, 1-18 (1990).
29. M. D. Thouless, A. G. Evans, M. F. Ashby, J. W. Hutchinson, The edge cracking and spalling of brittle plates. *Acta Metallurgica* **35**, 1333-1341 (1987).
30. L. Zhu *et al.*, Ice-phobic coatings based on silicon-oil-infused polydimethylsiloxane. *ACS applied materials & interfaces* **5**, 4053-4062 (2013).
31. F. Arianpour, M. Farzaneh, S. A. Kulinich, Hydrophobic and ice-retarding properties of doped silicone rubber coatings. *Applied Surface Science* **265**, 546-552 (2013).
32. Y. Wang *et al.*, Organogel as durable anti-icing coatings. *Science China Materials* **58**, 559-565 (2015).
33. D. L. Loughborough, E. G. Haas, Reduction of the Adhesion of Ice to De-Icer Surfaces. *Journal of the Aeronautical Sciences* **13**, 126-134 (1946).
34. J. W. Severin, R. Hokke, G. de With, Adhesion of electrolessly deposited Ni(P) layers on alumina ceramic. I. Mechanical properties. *Journal of Applied Physics* **75**, 3402-3413 (1994).
35. K. Golovin, A. Tuteja, A predictive framework for the design and fabrication of icephobic polymers. *Science Advances* **3**: e1701617 (2017).
36. A. Work, Y. Lian, A critical review of the measurement of ice adhesion to solid substrates. *Progress in Aerospace Sciences*, (2018).
37. P. Guo *et al.*, Icephobic/anti-icing properties of micro/nanostructured surfaces. *Adv Mater* **24**, 2642-2648 (2012).
38. J. Lv, Y. Song, L. Jiang, J. Wang, Bio-inspired strategies for anti-icing. *ACS nano* **8**, 3152-3169 (2014).
39. D. M. Cole, *ERDC/CRREL Nominal Mode I Ice Adhesion Testing*. (US Army Engineer Research and Development Center, Cold Regions Research and Engineering Laboratory (U.S.), (2014).
40. C. Wang, T. Fuller, W. Zhang, K. J. Wynne, Thickness dependence of ice removal stress for a polydimethylsiloxane nanocomposite: Sylgard 184. *Langmuir* **30**, 12819-12826 (2014).
41. E. T. Bowman, L. Susmel, The Theory of Critical Distances to model the short-to long-crack transition in geological materials subjected to Mode I static loading. *Procedia Materials Science* **3**, 562-567 (2014).

42. Q. Yang, M. Thouless, S. Ward, Numerical simulations of adhesively-bonded beams failing with extensive plastic deformation. *Journal of the Mechanics and Physics of Solids* **47**, 1337-1353 (1999).
43. E. Andrews, H. Majid, N. Lockington, Adhesion of ice to a flexible substrate. *Journal of materials science* **19**, 73-81 (1984).
44. M. Kafkalidis, M. Thouless, The effects of geometry and material properties on the fracture of single lap-shear joints. *International Journal of Solids and Structures* **39**, 4367-4383 (2002).
45. E. Andrews, N. Lockington, The cohesive and adhesive strength of ice. *Journal of materials science* **18**, 1455-1465 (1983).
46. M. S. Hu, M. D. Thouless, A. G. Evans, The decohesion of thin films from brittle substrates. *Acta Metallurgica* **36**, 1301-1307 (1988).
47. S. Clarson, K. Dodgson, J. Semlyen, Studies of cyclic and linear poly (dimethylsiloxanes): 19. Glass transition temperatures and crystallization behaviour. *Polymer* **26**, 930-934 (1985).

Acknowledgments:

Funding: We thank Dr. Ki-Han Kim and the Office of Naval Research (ONR) for financial support under grant N00014-12-1-0874. We also thank Dr. Kenneth Caster and the Air Force Office of Scientific Research (AFOSR) for financial support under grant FA9550-10-1-0523. We also thank the National Science Foundation and the Nanomanufacturing program for supporting this work through grant #1351412. K.G. thanks the Department of Defense (DoD) for a National Defense Science & Engineering Graduate (NDSEG) Fellowship, along with the Natural Sciences and Engineering Research Council of Canada for funding under grant RGPIN-2018-04272.

Author Contributions: K.G. and A.D. contributed equally. K.G. and A.D. designed and performed all experiments, wrote the manuscript. M.D.T., and A.T. conceived the research, designed experiments and wrote the manuscript.

Competing Interests: The University of Michigan has applied for a patent based on this technology. A startup company HygraTek LLC has licensed this technology from the University of Michigan. A.T. is the chief technology officer of, and has been a paid consultant, for HygraTek LLC.

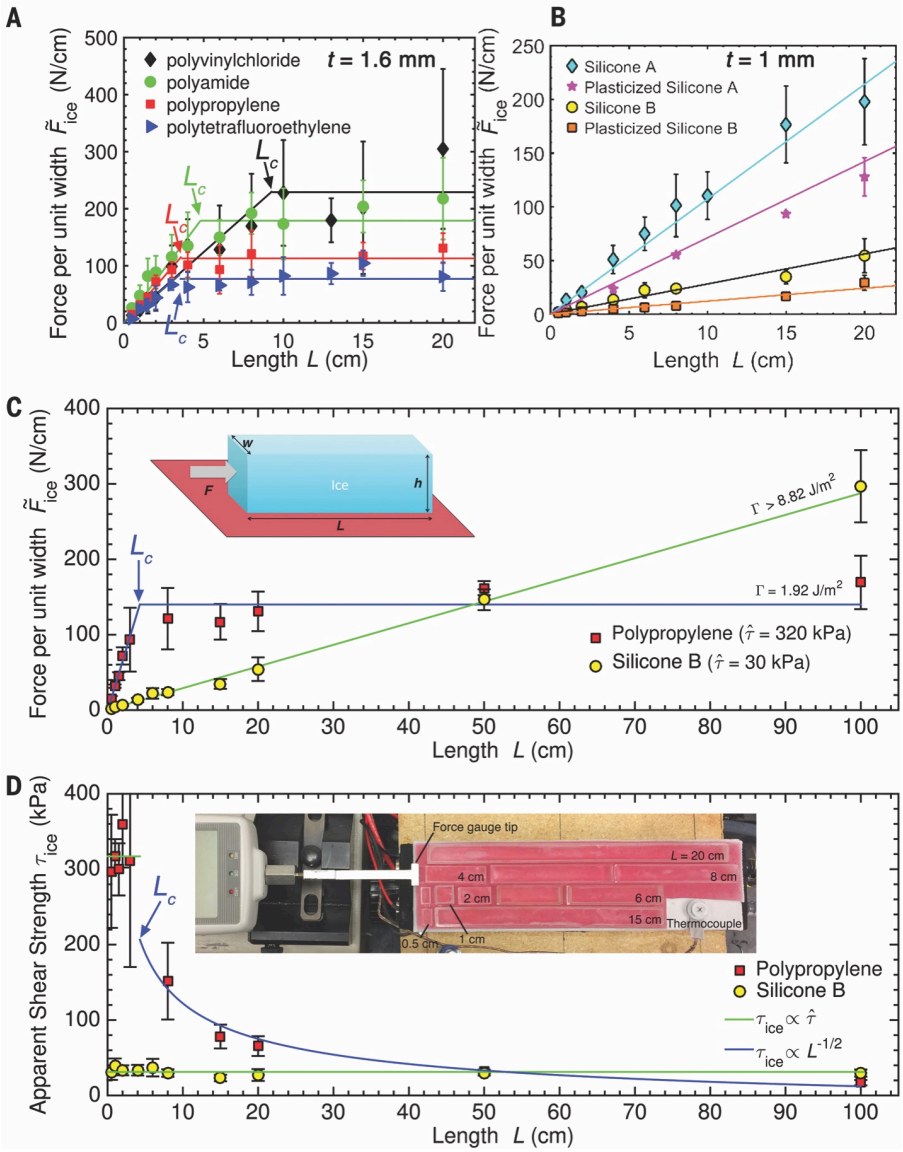

Figure 1. Strength- versus toughness-controlled fracture. (A) The force per unit width required to de-bond ice from four polymers (each 1.6 mm thick). Up to a critical length, L_c, the shear strength of the interface, $\hat{\tau}$, controlled the fracture of ice from these systems. However, after L_c, no additional force was necessary to remove the adhered ice. **(B)** The force per unit width required to de-bond ice from four silicones (thickness ~ 1 mm, section 1A in *(23)*). In all cases the fracture was controlled by the adhesive strength up to $L = 20$ cm, and no toughness-controlled fracture was observed. **(C)** The force per unit width required to de-bond ice from Silicone B and polypropylene (PP) as a function of interfacial length. For PP (thickness = 1.58 mm, section 1A in *(23)*), the force increased linearly with the length of ice until $L_c = 3.6$ cm, after which no additional force was required to remove the accreted ice. For Silicone B (thickness ~ 1 mm), strength always controlled the fracture even up to 100 cm. The inset shows a schematic of the situation being investigated. **(D)** Data from **C** recast in terms of the apparent shear strength, τ_{ice}, indicating that τ_{ice} for Silicone B is less than that of PP only when $L \leq 50$ cm. The inset shows our experimental setup, with 11 pieces of ice of 8 different lengths adhered to Silicone B. All experiments shown were conducted at -10 °C. Error bars denote 1 standard deviation ($N \geq 5$).

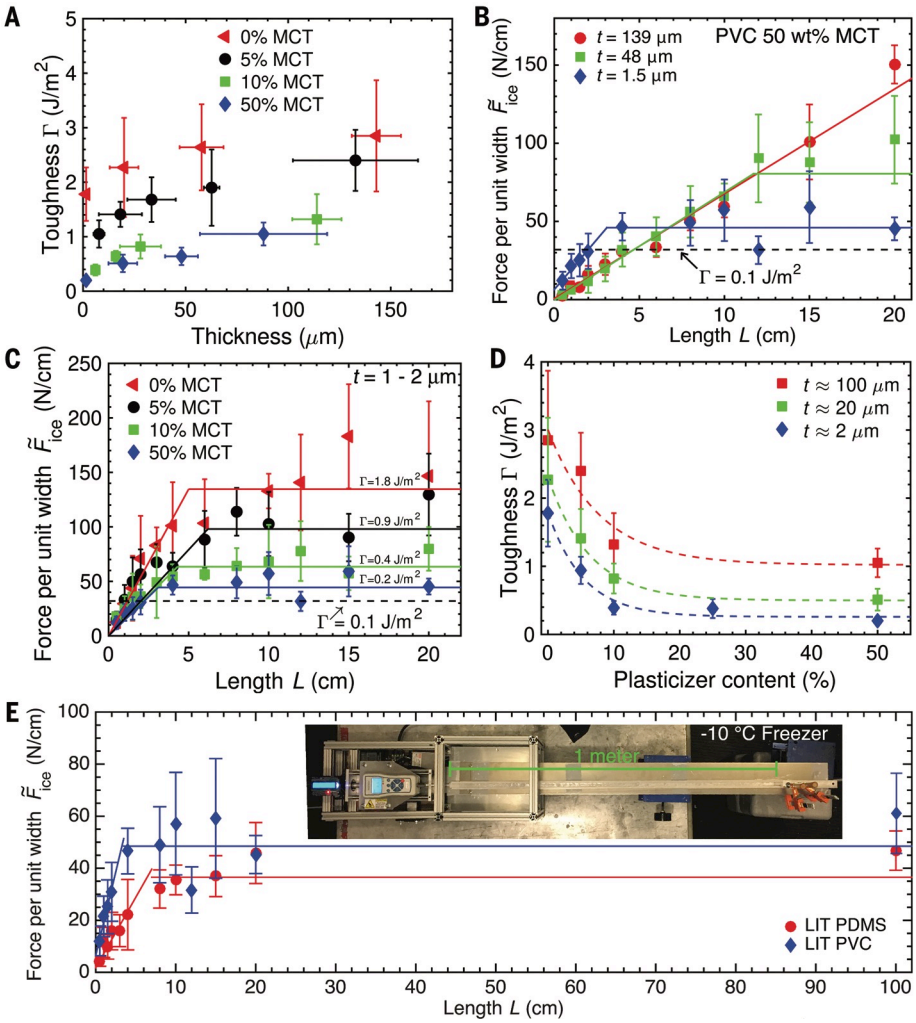

Figure 2. Controlling interfacial toughness. **(A)** The effect of coating thickness on the effective interfacial toughness between an aluminum substrate coated with plasticized PVC, and ice, for four different plasticizer contents. **(B)** The force per unit width required to fracture ice from three different thickness of PVC plasticized with 50 wt% medium-chain triglyceride (MCT) oil. Note that, for the thickest sample, strength controlled the fracture up to at least $L = 20$ cm. **(C)** The force per unit width required to fracture ice from thin ($t \approx$ 1-2 μm) PVC coatings with four different plasticizer contents. A toughness-controlled regime of fracture was always observed for lengths less than 20 cm. **(D)** The effect of plasticizer content on Γ for three different thicknesses of plasticized PVC. All experimental results shown were obtained at -10 °C. **(E)** The force required to fracture ice from the LIT PDMS and LIT PVC systems (thickness ≈ 1-2 μm). Even over an interfacial length of 1 meter, the necessary force of fracture remained constant beyond L_c. The inset shows our experimental setup, performed in a walk-in freezer at - 10 °C. Error bars denote 1 standard deviation ($N \geq 5$).

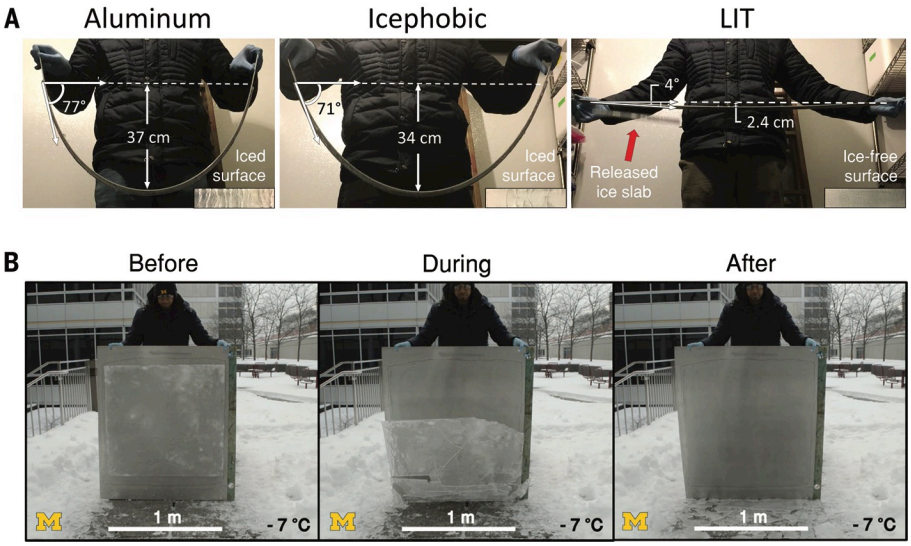

Figure 3. Large scale testing of LIT materials. (A), A comparison between uncoated, icephobic, and LIT aluminum beams adhered to a sheet of ice (100 cm × 2.5 cm × 0.8 cm) undergoing off-center load flex tests inside a walk-in freezer held at -20 °C (section 1B in *(23)*). Ice fractured from the LIT-coated specimen with a remarkably low apparent ice adhesion strength of 0.39 kPa, while ice remained adhered to the uncoated aluminum and icephobic specimens even at severe deflections (Movie S2). **(B)**, An aluminum sheet coated with LIT PDMS before, during, and after fracture from a large sheet of ice (0.95 m × 0.95 m × 0.01 m). The weight of the ice sheet alone was sufficient to cause fracture, displaying an exceedingly low apparent ice adhesion strength of 0.09 kPa. A comparison is also made to uncoated aluminum (Movie S5).

Surface	$\theta_{rec}/\theta_{adv}$ (water)	$\hat{\tau}$ (kPa)	τ_{ice} (kPa) at $L = 20$ cm	L_c (cm)	$\tilde{F}_{ice}^{cr}$ (N/cm)	Γ (J/m^2)	E (GPa)
Silicone A	120°/87°	107 ± 12	107 ± 12	≥ 20	≥ 198	≥ 3.8	$3.5 \pm 1.2 \times 10^{-1}$
Plasticized Silicone A	112°/102°	55 ± 11	55 ± 11	≥ 20	≥ 128	≥ 1.6	$2.7 \pm 0.33 \times 10^{-2}$
Silicone B	113°/96°	29 ± 2	29 ± 2	≥ 100	≥ 297	≥ 8.7	$5.3 \pm 0.99 \times 10^{-4}$
Plasticized Silicone B	115°/86°	12 ± 2	12 ± 2	≥ 100	≥ 126	≥ 1.6	$1.2 \pm 0.14 \times 10^{-4}$
PVC	92°/63°	248 ± 52	114 ± 26	9.3 ± 2.2	229 ± 52	5.1 ± 2.3	3.6 ± 0.11
PC	92°/69°	302 ± 20	103 ± 11	6.5 ± 0.7	207 ± 22	4.2 ± 0.90	3.3 ± 0.01
Nylon	53°/15°	373 ± 99	89 ± 11	4.8 ± 1.7	179 ± 22	3.1 ± 0.76	3.4 ± 0.15
ABS	99°/59°	177 ± 54	86 ± 30	10 ± 4.0	174 ± 23	3.0 ± 0.79	2.9 ± 0.07
PMMA	78°/52°	280 ± 45	121 ± 11	6.2 ± 1.2	170 ± 22	2.8 ± 0.72	3.3 ± 0.18
PETG	89°/62°	251 ± 49	84 ± 20	6.8 ± 1.8	169 ± 40	2.8 ± 1.3	3.7 ± 0.01
CPVC	99°/55°	309 ± 39	67 ± 7	5.6 ± 0.5	133 ± 39	1.7 ± 0.37	2.6 ± 0.07
PP	104°/86°	322 ± 42	64 ± 5	3.6 ± 0.7	127 ± 10	1.6 ± 0.26	3.0 ± 0.53
Garolite	85°/35°	317 ± 58	70 ± 29	4.2 ± 1.0	124 ± 16	1.5 ± 0.39	4.2 ± 0.07
PS	103°/64°	151 ± 20	76 ± 25	8.1 ± 1.4	120 ± 17	1.4 ± 0.40	3.0 ± 0.07
LDPE	108°/83°	238 ± 27	52 ± 6	4.6 ± 0.6	105 ± 12	1.1 ± 0.24	1.0 ± 0.10
UHMWPE	103°/76°	234 ± 27	49 ± 5	3.8 ± 0.4	97 ± 10	0.9 ± 0.19	1.9 ± 0.04
PTFE	123°/91°	241 ± 36	39 ± 4	3.5 ± 0.7	77 ± 8	0.6 ± 0.12	0.2 ± 0.03
LIT PS	104°/82°	141 ± 54	30 ± 3	4.5 ± 2.8	66 ± 6	0.43 ± 0.08	$5.9 \pm 1.0 \times 10^{-4}$
LIT PVC	97°/77°	107 ± 13	23 ± 4	4.3 ± 0.9	52 ± 7	0.27 ± 0.07	$1.2 \pm 0.04 \times 10^{-1}$
LIT PDMS	113°/96°	115 ± 48	18 ± 2	6.7 ± 3.2	35 ± 4	0.12 ± 0.03	$1.2 \pm 0.14 \times 10^{-4}$
Pure Van der Waals	–	–	–	–	32 (calc.)	0.10	–

Table 1. Values for interfacial properties measured between ice and 20 different surfaces. A comparison is made between 1-mm thick coatings of icephobic silicones on aluminum, 1.58-mm thick plastic substrates, and 1-2 μm thick LIT coatings on aluminum (see section 1A in *(23)* for fabrication and composition descriptions). $\tilde{F}_{ice}^{cr}$ for pure van der Waals interaction was calculated using $\Gamma = 0.1$ J/m^2 (*5, 34*) for a 6 mm thick ice sheet. Data uncertainty denotes 1 standard deviation ($N \geq 5$).